Structure of Bleomycin-Induced DNA Double-Strand Breaks: Predominance of Blunt Ends and Single-Base 5′ Extensions†

Lawrence F. Povirk,* Yi-Hong Han, and Robert J. Steighner

Department of Pharmacology and Toxicology, Medical College of Virginia, Virginia Commonwealth University, Richmond, Virginia 23298

Received January 19, 1989; Revised Manuscript Received March 30, 1989

ABSTRACT: In order to examine the structure of bleomycin-induced DNA double-strand breaks, defined-sequence DNA was labeled in each strand at a single restriction site and treated with bleomycin. Various double-stranded fragments resulting from bleomycin-induced double-strand breaks were isolated, denatured, and run on sequencing gels to determine the sites of cleavage in each strand. For virtually every double-strand break, the cleavage site in one strand was a pyrimidine in a G-Py sequence, reflecting a specificity similar to that of bleomycin-induced single-strand cleavage. However, the cleavage site in the complementary strand was seldom a G-Py sequence, and was usually a site where single-strand cleavage was infrequent. When the sequence at the double-strand break was G-Py-Py′, the break at Py was usually accompanied by a break at the base directly opposite Py, resulting in blunt ends. When the sequence was G-Py-Pu, the break at Py was usually accompanied by a break at the base opposite Pu, resulting in single-base 5′ extensions. Double-strand breaks with 3′ extensions, such as would result from cleavage of two C residues in a self-complementary G-C sequence, were conspicuously absent. These data provide further evidence that bleomycin-induced double-strand breaks do not result from coincidence of independent site-specific single-strand breaks. A model is proposed wherein Fe(III)·bleomycin and a 4′-peroxyl derivative of deoxyribose, both formed during cleavage at the G-*Py* site, combine to regenerate activated bleomycin, which then effects a second cleavage at a specific site in the complementary strand, either directly opposite *Py* or opposite the base one position downstream.

The glycopeptide antibiotic bleomycin produces double-strand breaks in DNA with a frequency far in excess of that expected from coincidence of single-strand breaks (Povirk et al., 1977; Lloyd et al., 1978a,b). However, the chemistry of activated bleomycin provides no suggestion of bifunctionality (Burger et al., 1981), and the mechanism of double-strand cleavage has remained obscure.

The precise structure of bleomycin-induced double-strand breaks and, in particular, the relative positions of the breaks in complementary strands have never been definitively determined. Since *C* and *T* residues in G-*C* and G-*T* sequences are the most frequent sites of bleomycin attack (D'Andrea & Haseltine, 1978; Takeshita et al., 1978), and since the double-strand breaks appear to occur at or near G-C sequences, coincident cleavage of the two C residues in this self-complementary sequence has been proposed as a mechanism of double-strand cleavage (Mirabelli et al., 1982). However, other studies, suggesting that the breaks leave two base pair cohesive ends (Lloyd et al., 1979), would appear to be inconsistent with this proposal.

In this report, we show that, at low cleavage levels, most bleomycin-induced double-strand breaks have either blunt ends or noncomplementary single-base 5′ extensions and that the positions of the breaks differ markedly from what would be predicted from the pattern of single-strand breaks in each strand. The results suggest that there is a phenomenological link between the two cleavage events comprising each double-strand break. A specific model is proposed to account for these and other features of bleomycin-induced double-strand cleavage of DNA.

† This work was supported by Grant CA40615 from the National Cancer Institute, DHHS.

* Author to whom correspondence should be addressed.

Materials and Methods

Materials. Plasmid DNAs were prepared by the alkaline lysis method and banded twice in CsCl–ethidium bromide gradients. Various fragments were labeled at the 3′ end with the Klenow fragment of DNA polymerase I and an appropriate deoxynucleotide [α-^{32}P]triphosphate, or at the 5′ end with polynucleotide kinase and [γ-^{32}P]ATP (exchange reaction). When 3′ or 5′ end-labeling was performed at restriction sites having 5′ extensions, the 3′ termini were always completely filled in by the Klenow fragment (Maniatis et al., 1980).

Three defined-sequence fragments were used. The first was from a segment of the λ *c*I gene (bases 167–714, plus 555 bp of downstream DNA sequence) which was cloned as an *Nsi*I fragment into the *Pst*I site in the polylinker region of pUC19. This recombinant plasmid was cut in the polylinker with *Sal*I, labeled at the *Sal*I site, and digested with *Rsa*I, releasing a 149 bp fragment which contained bases 167–310 of *c*I and was end-labeled (in the polylinker) at the equivalent of base 162. The second fragment consisted of bases 886–959 of the *lacI* gene. the 789 bp *Hin*cII fragment of the *lacI*-containing plasmid pMC1 was isolated, 3′ or 5′ end-labeled, and digested with *Bst*NI, releasing a 74 bp fragment labeled at the *Hin*cII site. Alternatively, the unlabeled 74 bp fragment was first isolated and then selectively labeled at the *Bst*NI site with Klenow fragment and [α-^{32}P]dATP. The third fragment was a 377 bp *Bam*HI/*Eco*RI fragment, containing bases 3–379 of pBR322 (*tet* gene) and similarly 3′ or 5′ end-labeled at the *Bam*HI site.

Purified bleomycin A_2 was a gift of Dr. W. T. Bradner, Bristol Laboratories. Fe(III)·bleomycin was prepared as described previously (Povirk & Houlgrave, 1988) and stored at −20 °C at a concentration of 1 mM.

Bleomycin–DNA Reactions. Reaction mixtures (20–30 μL) contained 20 μg/mL sonicated calf thymus DNA, a ^{32}P-

0006-2960/89/0428-5808$01.50/0

end-labeled fragment (<10 μg/mL), 0–1 μM Fe(III)·bleomycin, 25 mM 2-mercaptoethanol, 50 mM *N*-(2-hydroxyethyl)piperazine-*N*′-2-ethanesulfinic acid–potassium hydroxide (Hepes–KOH),[1] pH 8, and 0.1 mM EDTA. Bleomycin, diluted immediately before use, was added last. EDTA, which did not inhibit bleomycin at this concentration, was included to chelate any trace metal contaminants. Mixtures were incubated at 37 °C for 30 min. Following addition of one-fifth volume of 40% sucrose–0.1 M EDTA–0.2% bromophenol blue, the samples were immediately electrophoresed on nondenaturing gels.

Electrophoresis. Nondenaturing gels (30 × 40 × 0.8 cm) contained 12% polyacrylamide [29:1 acrylamide:bis(acrylamide) ratio], 16 mM Hepes–NaOH, pH 7.5, 16 mM sodium acetate, and 0.8 mM EDTA. Gels were run at 240 V for approximately 24 h at 4 °C ambient temperature. Recirculation between anode and cathode reservoirs was required to maintain buffer pH.

Following autoradiography for 1–2 days at 4 °C, bands corresponding to bleomycin-induced double-strand breaks were excised from the gel. Each gel slice was cut into several pieces, placed in 3 mL of 0.3 M sodium acetate–1 μg/mL tRNA–1 mM EDTA, and agitated for 16 h to elute the DNA. The eluate was evaporated to approximately 0.4 mL, and the DNA was ethanol-precipitated, dissolved in 20 μL of 80% formamide containing 10 mM EDTA, pH 8, and run on an 8% or 12% polyacrylamide denaturing sequencing gel along with appropriate markers (Maxam & Gilbert, 1979). Alternatively, the precipitated DNA was dissolved in 50 mM Tris (pH 9)–1 mM $MgCl_2$–0.1 mM $ZnCl_2$–1 mM spermidine and treated with calf intestinal phosphatase (1 h, 37 °C, 100 units/mL) or dissolved in 0.1 M MES–NaOH (pH 5.5)–1 mM $MgCl_2$ and treated with T4 polynucleotide kinase (16 h, 37 °C, 500 units/mL). Under these conditions, polynucleotide kinase specifically removes phosphates from the 3′ ends of polynucleotides (Cameron & Uhlenbeck, 1977). Phosphatase-treated samples were reprecipitated prior to sequencing gel analysis.

Results

Determination of Double-Strand Cleavage Sites. In order to determine unequivocally the cleavage sites involved in double-strand breaks, identical defined-squence fragments, labeled independently in each strand at a single restriction site, were prepared. As shown by analysis on nondenaturing gels (Figure 1), treatment of these fragments with low concentrations of bleomycin produced a number of discrete shorter double-stranded fragments, indicating formation of site-specific double-strand breaks by the drug. As expected, identical patterns were seen with the 3′ and 5′ end-labeled molecules. Each major, well-defined band was then excised from the gel, and this DNA was eluted, denatured, and rerun on a denaturing sequencing gel. In this way, it was possible to determine the cleavage sites in each strand for each of the double-stranded fragments generated by bleomycin treatment. Portions of sequencing gels analyzing some of the double-strand breaks formed in the *c*I gene fragment are shown in Figure 2. For each band isolated from the nondenaturing gel, there was a single predominant site of cleavage in each strand. The 3′ end-labeled polynucleotides derived from the bleomycin-treated DNA exactly comigrated with the 5′-phosphate-ended Maxam–Gilbert markers, suggesting that, as expected, the bleomycin-induced breaks had 5′-phosphate termini (Kuo & Haidle, 1974). Removal of the 5′-phosphate from the polynucleotides with calf intestinal phosphatase prior to sequencing gel analysis produced the expected decrease of approximately one nucleotide position in the mobility of the labeled polynucleotides (not shown). The 5′ end-labeled polynucleotides derived from bleomycin-treated DNA migrated just ahead of the 3′-phosphate-ended markers, a characteristic property of polynucleotides with the 3′-phosphoglycolate terminus produced by bleomycin (D'Andrea & Haseltine, 1978; Takeshita et al., 1978; Giloni et al., 1981). As expected, the mobility of these 5′ end-labeled polynucleotides was not affected by alkaline treatment, or by treatment with polynucleotide kinase under conditions where 3′-phosphates were efficiently removed from Maxam–Gilbert markers (not shown).

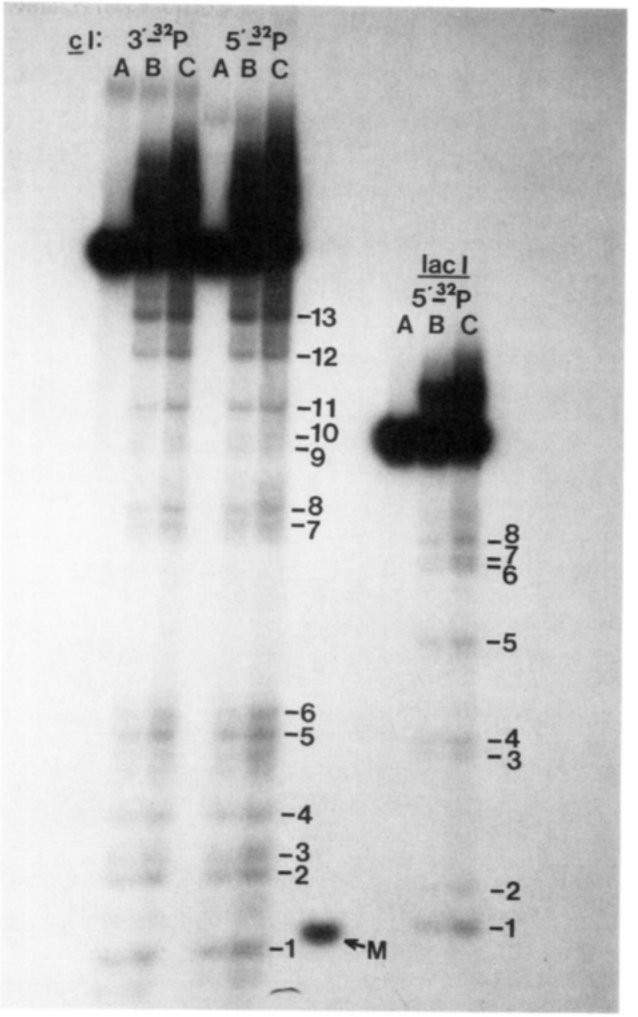

FIGURE 1: Double-strand cleavage of end-labeled DNA by bleomycin. The 149 bp *c*I and 74 bp *lacI* DNA fragments, bearing 5′ or 3′ end-label as indicated, were treated with 0 (A), 0.3 (B), or 1.0 (C) μM bleomycin and electrophoresed on a nondenaturing gel. Numbers show fragments which were eluted for determination of cleavage sites. The band marked "M" is a 24 bp double-stranded marker.

Figure 3 summarizes the 26 double-strand cleavage sites determined in 3 defined-sequence DNA fragments (from the *c*I, *lacI*, and *tet* genes). Cleavage sites are analyzed in more detail below, but the most striking feature was that, for the majority of double-strand breaks, the breaks either were directly opposite, resulting in blunt ends (11 sites), or were staggered by 1 base, resulting in single-base 5′ extensions (12 sites). There were few if any breaks with 3′ extensions.

In order to check for possible artifacts in the determination of cleavage sites, one strand of the *lacI* fragment (upper strand in Figure 3) was labeled independently at both ends, and DNA

[1] Abbreviations: Hepes, *N*-(2-hydroxyethyl)piperazine-*N*′-2-ethanesulfonic acid; MES, 2-(*N*-morpholino)ethanesulfonic acid.

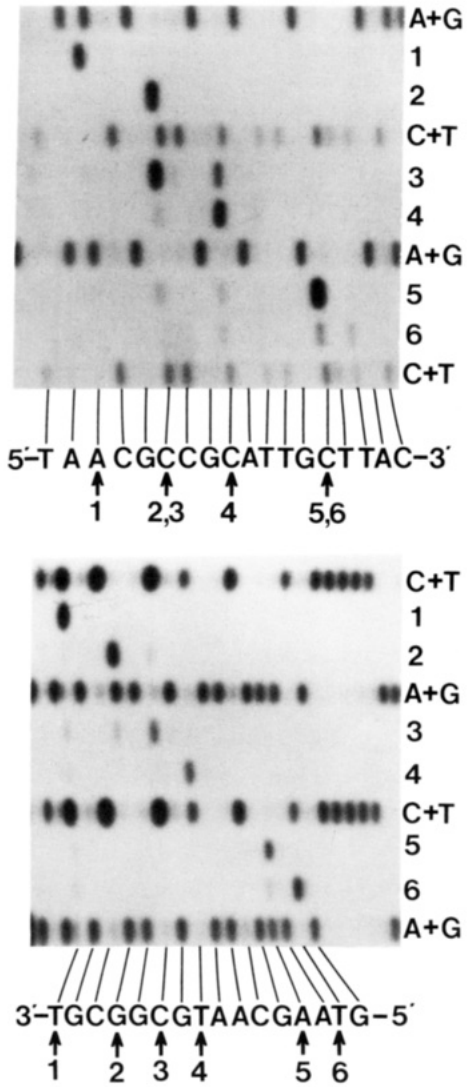

FIGURE 2: Determination of sites of double-strand cleavage in the 5′ end-labeled (top) or 3′ end-labeled (bottom) strands of the *c*I fragment. Numbered bands from Figure 1 were eluted, denatured, and electrophoresed on denaturing sequencing gels. "A+G" and "C+T" lanes are Maxam–Gilbert markers. The top of the gel is to the right.

with each label was treated with bleomycin and run on a nondenaturing gel. In each case, eight major sites of double-strand cleavage were detected (5′ end-label shown in Figure 1; 3′ end-label not shown), and the break sites as determined from opposite ends of the strand were identical. These results, combined with the phosphatase data, suggest that misidentification of cleavage sites due to unusual termini or other artifacts is unlikely.

Similar patterns of double-strand cleavage were obtained at the two bleomycin concentrations used in Figure 1. However, there were a few rather diffuse bands which appeared only at the higher concentration (e.g., between bands 4 and 5 of the *c*I fragment), and which became more prominent at even higher concentrations (not shown). Sequencing gel analysis revealed that each of these diffuse bands reflected cleavage at multiple sites in both strands and that a high proportion of these sites were G-*Py* sequences. This specificity suggests that the diffuse bands represent bona fide coincidences between closely opposed single-strand breaks, which would be expected to dominate the double-strand cleavage pattern at sufficiently high levels of DNA damage.

Comparison with Single-Strand Cleavage Sites. Previous work has shown that bleomycin-induced single-strand breaks occur primarily at pyrimidines in G-*C* and G-*T* sequences (D'Andrea & Haseltine, 1978; Takeshita et al., 1978). The results shown in Figure 3 suggest that double-strand breaks have a somewhat different specificity. In most cases, only one break of each double-strand break occurred at a G-*Py* site; the break in the opposite strand appeared to have much weaker sequence specificity. In order to compare double-strand and single-strand cleavage sites, the labeled *c*I and *lacI* fragments shown in Figure 3 were treated with bleomycin, denatured, and run directly on a denaturing sequencing gel; since single-strand breaks are 9 times more frequent than double-strand breaks (Povirk et al., 1977), this procedure should produce a pattern reflecting predominantly the specificity of single-strand cleavage.

Results obtained with the 3′ end-labeled *c*I gene fragment are shown in Figure 4, and similar patterns were seen in both strands of both fragments. Strong single-strand cleavage was detected at each of the G-*C* and G-*T* sites involved in double-strand cleavage (e.g., sites 1, 3, and 6 in Figure 4), while at the other major sites of double-strand cleavage (sites 2, 4, and 5) only weak single-strand cleavage was seen. Thus, for most of the double-strand breaks, it was possible to define a primary cleavage site, with sequence G-*Py*, and a secondary cleavage site, with a sequence other than G-Py. As discussed below, the primary break probably occurs before the secondary break.

Specificity of the Secondary Cleavage Sites. The sequence specificity for the primary (G-*Py*) cleavage site of each double-strand break reflected the previously determined specificity of single-strand cleavage, and will not be considered in detail. However, analysis of the secondary breaks revealed a distinctly different set of ordered specificities. The most important of these specificities was in the positioning of the secondary break with respect to the primary break. With the exception of the few double-strand breaks involving two closely opposed G-*Py* sites, each secondary break occurred either directly opposite the primary break (producing blunt ends) or opposite the base to the 3′ side (downstream) of the break (producing single-base 5′ extensions). Analysis of 23 such double-strand breaks (Table I) indicated that in most cases the selection between these two secondary sites was determined by one of two factors: the preference for a pyrimidine at the secondary cleavage site, as in sequences of the form

```
        ↓
5′-G-Py-Pu-Pu-3′
3′-C-Pu-Py-Py-5′
        ↓
```

and the preference for a purine to the 5′ side of the site, as in sequences of the form

```
        ↓
5′-G-Py-Py-Pu-3′
3′-C-Pu-Pu-Py-5′
        ↓
```

(primary cleavage site shown in upper strand, secondary site in lower strand). Because these two specificities are never in conflict, it could not be determined which was stronger. However, each of them was always fulfilled whenever the sequence allowed. In sequences of the form

```
        ↓
5′-G-Py-Py-Py-3′
3′-C-Pu-Pu-Pu-5′
      (↓) (↓)
```

where each of the two potential cleavage sites was a purine flanked on the 5′ side by another purine, weaker specificities came into play. When one of the two sites was an adenine,

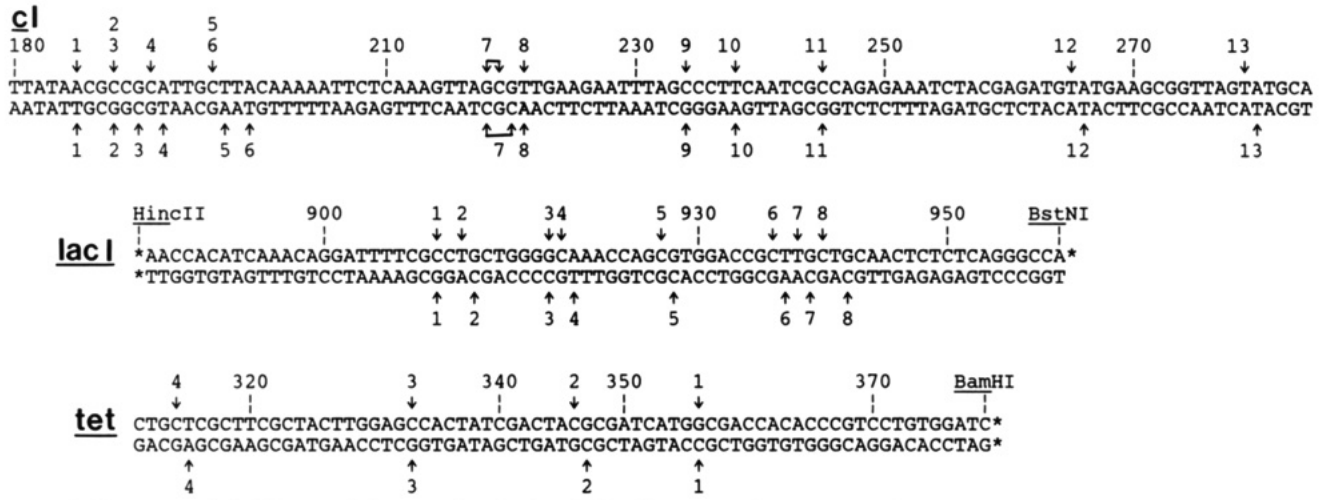

FIGURE 3: Summary of double-strand cleavage sites in three DNA fragments. Sequences read 5′ to 3′ in the top strand and 3′ to 5′ in the bottom strand. Sites were determined as described in Figures 1 and 2. The positions of end-labeling for the *lacI* and *tet* gene fragments are indicated by asterisks; the *c*I fragment was labeled in each strand at base 162. Each of the bands eluted from the nondenaturing gels gave, for each type of end-label, a single predominant band on nondenaturing gels except for band 7 of the *c*I fragment, which gave two bands of comparable intensity; by analogy to other cleavage sites, it was assumed to result from two adjacent double-strand cleavage sites with zero- and one-base stagger. In the case of the *tet* gene fragment, only double-strand breaks within 70 bp of the labeled end were analyzed.

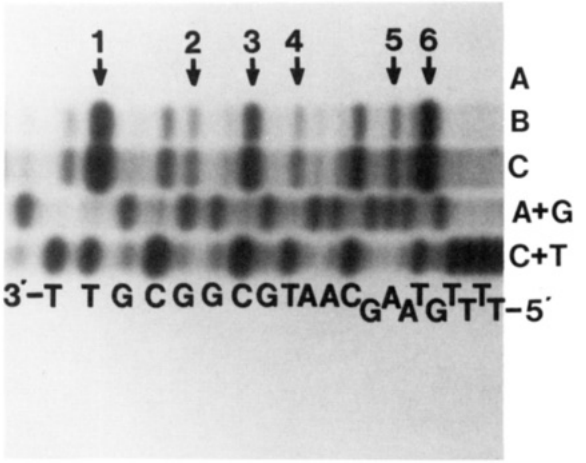

FIGURE 4: Bleomycin-induced single-strand cleavage of the 3′ end-labeled *c*I fragment. The fragment was treated with 0 (A), 0.3 (B), or 1.0 (C) μM bleomycin, denatured, and electrophoresed on a denaturing sequencing gel. The top of the gel is to the right. The numbers show the sites of double-strand cleavage (see Figure 3). Note that several of the major double-strand cleavage sites (2, 4, and 5) were only minor sites of single-strand cleavage.

that site was preferred; when both were guanines, the site directly opposite the primary break was preferred (see Table I).

It is notable that, despite these multiple overlapping specificities, not a single sequence was found where secondary cleavage occurred at both potential sites. Rather, the position of each secondary cleavage site was uniquely determined by a hierarchy of selection rules. These rules can be seen as a modification of the specificity of bleomycin-induced single-strand cleavage, relaxed as necessary to permit cleavage at one of the two potential secondary sites. The preference for pyrimidines over purines and for adenine over guanine at secondary cleavage sites reflects the base specificity of bleomycin-induced single-strand cleavage [T > C > A > G (Takeshita et al., 1981)], while the preference for a purine 5′ to the secondary cleavage site can be seen as a remnant of the requirement for a guanine to the 5′ side of single-strand cleavage sites.

A special minor class of double-strand breaks, for which primary and secondary breaks could not be distinguished,

Table I: Compilation of Sites of Bleomycin-Induced Double-Strand Cleavage[a]

general form	sequence (occurrences)				
G-Py-Py-Pu C-Pu-Pu-Py	GCCA CGGT (3)	GCCG CGGC	GCTA CGAT	GTTA CAAT	GTTG CAAC
G-Py-Py-Py C-Pu-Pu-Pu	GCCC CGGG (2)	GCCT CGGA			
	GCTT CGAA (2)	GCTC CGAG			
G-Py-Pu-Py C-Pu-Py-Pu	GCGT CGCA (3)	GTAT CATA (2)	GCAT CGTA		
G-Py-Pu-Pu C-Pu-Py-Py	GCAA CGTT (2)	GCAG CGTC			
G-Py-N-Pu-C C-Pu-N-Py-G	GCCGC CGGCG	GCTGC CGACG			
Other	GCTTAC CGAATG	GAAG CTTC			

[a] Double-strand cleavage sites in the three restriction fragments have been arranged according to sequence and stagger, as shown in the left-hand column. Arrows show positions of breaks. The primary (G-*C* or G-*T*) cleavage site is shown in the top strand and the secondary site in the bottom strand. Sequences read 5′ to 3′ in the top strand and 3′ to 5′ in the bottom strand.

consisted of those involving cleavage at two closely opposed G-*Py* sequences. These were the only breaks which had two- or three-base stagger, producing two- or three-base 5′ extensions (Table I, bottom). Although the breaks in both strands occurred at prominent sites of single-strand clevage, it is unlikely that these double-strand breaks were simply coincidences of single-strand breaks, since no double-strand breaks with 3′

extensions were detected, even when nearby G-*Py* sequences were available in both strands. Thus, it is likely that, compared to the breaks with zero- or one-base stagger, these double-strand breaks represent an alteration in specificity rather than in mechanism, with the preference for G-*Py* sequences overriding the preference for a minimum stagger between primary and secondary breaks. However, the preference for G-*Py* sites did not overcome the prohibition against double-strand breaks with 3′ extensions of any length. In particular, there were few if any double-strand breaks involving two C residues in a self-complementary G-C sequence, even in cases where both were prominent sites of single-strand cleavage. The strength of this specificity was evident at sequences such as that at sites 3 and 4 in the *lacI* fragment, where two such C residues were each involved in separate double-strand breaks, but were never involved in the *same* double-strand break.

It is important to note that, for each bleomycin-induced cleavage, one base and most of its sugar are eliminated. Thus, at the staggered double-strand breaks, the 5′ extensions are usually noncomplementary, and at the blunt-ended breaks, one complete complementary base pair is lost.

Discussion

Mechanism of Double-Strand Cleavage. Models for bleomycin-induced double-strand cleavage must reconcile two conflicting bodies of evidence. On one hand, double-strand cleavage of supercoiled DNA by bleomycin shows kinetics expected for a "one-hit" process, with the fraction of linear molecules increasing linearly over time and with the ratio of double- to single-strand breaks (approximately 1:9) remaining invariant over a wide range of bleomycin concentrations (Povirk et al., 1977; Lloyd et al., 1978a,b). These results suggest that double-strand breaks result from a single interaction between bleomycin and DNA. On the other hand, the chemistry of activated bleomycin (Burger et al., 1981; Kuramochi et al., 1981; Hecht, 1986) provides no suggestion of bifunctionality, suggesting that two bleomycin–DNA interactions should be required for each double-strand break.

In agreement with the earlier kinetic data, our results strongly suggest that double-strand breaks are not coincidences of independent site-specific single-strand breaks. The fact that the secondary cleavage sites display a specificity markedly different from that of bleomycin-induced single-strand cleavage strongly suggests that the primary and secondary cleavage events are intimately, phenomenologically linked. At the same time, the findings that (i) both the primary and the secondary breaks possess 5′-phosphate and 3′-phosphoglycolate termini and (ii) the secondary cleavage sites retain some features of normal bleomycin specificity suggest that the secondary as well as the primary break results from specific attack on C-4′ by an activated bleomycin molecule (rather than, for example, by a diffusible hydroxyl radical generated during the primary cleavage event).

On the basis of these considerations, we propose the following model of bleomycin-induced double-strand cleavage: (i) a molecule of activated bleomycin first attacks DNA at the primary (G-*C* or G-*T*) cleavage site; (ii) the Fe(III)·bleomycin generated as a product of this attack (Burger et al., 1981) and the 4′-peroxyl derivative of deoxyribose generated as an intermediate in the cleavage reaction (Giloni et al., 1981) combine to regenerate activated bleomycin; (iii) this activated bleomycin molecule immediately, without dissociating from DNA, undergoes a rearrangement in binding and effects a secondary attack in the complementary strand, at a site whose position is determined primarily by the position of the first break; (iv) breaks with 5′-phosphate and 3′-phosphoglycolate termini are thus produced at both the primary and the secondary cleavage sites, resulting in a double-strand break. That organic peroxides, as well as hydrogen peroxide, can combine with Fe(III)·bleomycin to form activated bleomycin has been recently demonstrated by Padbury et al. (1988).

While the evidence for this model is indirect, the model does explain some otherwise puzzling features of bleomycin-induced double-strand cleavage. Since it involves, in a kinetic sense, only a single bleomycin–DNA interaction, it predicts the observed single-hit kinetics for double-strand break formation. To explain the fact that only 10% of breaks are double-strand breaks, it need only be postulated that certain steps involved in secondary cleavage, e.g., the regeneration of activated bleomycin, are less that 100% efficient. The model also explains the observation that bleomycin induces direct double-strand breaks and AP sites with closely opposed breaks, but no double closely opposed AP sites (Povirk & Houlgrave, 1988). AP sites with closely opposed breaks could occur if, as expected, the secondary attack sometimes partitions into an AP site rather than a strand break (Wu et al., 1985). However, if the primary attack partitions into an AP site, the 4′-peroxyl intermediate would not be formed, activated bleomycin could not be regenerated, and secondary attack could not occur. Thus, double closely opposed AP sites would never be formed. The model predicts, then, that the AP site in a bivalent AP site/strand break lesion will always occur at the secondary site, a prediction we are currently testing.

In theory, the activated bleomycin needed for secondary cleavage could be regenerated from Fe(III)·bleomycin by sulfhydryls plus oxygen. However, the reduction of Fe(III)·bleomycin by sulfhydryls is a relatively slow reaction (Povirk, 1979), and the fact that the ratio of double- to single-strand breaks is the same in the presence and absence of sulfhydryls (Hutchinson & Povirk, 1979) argues that regeneration of activated bleomycin by the reaction of Fe(III)·bleomycin with the 4′-peroxide is a more likely pathway.

An alternative model of double-strand cleavage is that the one-base gap formed at the primary break renders the complementary strand extremely susceptible to cleavage at the secondary site by a second molecule of activated bleomycin. Using synthetic substrates, Keller and Oppenheimer (1987) have in fact shown that a one-base gap with 3′- and 5′-phosphate termini (a structure nearly identical with a bleomycin-induced single-strand break) dramatically increased the extent of bleomycin-induced cleavage at the nucleotide directly opposite the gap. However, while this model predicts both a high-frequency of double-strand breaks and an altered specificity for secondary cleavage sites, as well as the specific salt suppression of double-strand cleavage (Lloyd et al., 1978b), it does not readily explain the constant ratio of double- to single-strand breaks. Even if the presence of the primary break markedly increases the probability of secondary attack, it is difficult to escape the conclusion that the ratio of double- to single-strand brakes should increase with increasing bleomycin damage, since the number of targets for double-strand cleavage (i.e., existing single-strand breaks) increases while the number of targets for single-strand cleavage remains constant. Thus, unless some unusual and as yet undetermined feature of the reaction kinetics can be invoked to explain the constant ratio of double- to single-strand breaks, the kinetic data strongly favor a model which involves interaction of only a single bleomycin molecule with DNA. However, the specific binding of bleomycin at the charged gap formed by the primary break, as suggested by the results of Keller and Oppenheimer, could

be important in preventing dissociation of bleomycin during reactivation and secondary cleavage, as well as in positioning the regenerated activated bleomycin for secondary clevage at a specific site in the complementary strand.

Comparison with Other Antibiotics. Neocarzinostatin (Povirk & Houlgrave, 1988) and calicheamicin (Zien et al., 1988) have also been shown to produce a large proportion of double-strand breaks and/or abasic sites with closely opposed strand breaks, in DNA. However, both the geometry and the chemistry of the breaks appear to be quite different from those of the bleomycin-induced breaks. Neocarzinostatin and calicheamicin both contain diyne-ene ring structures which are believed to be converted by sulfhydryls into biradical species. These biradicals probably abstract two hydrogens simultaneously from two sugars which lie directly across from each other in the minor groove, resulting in staggered double-strand breaks (or AP sites with closely opposed strand breaks) with two-base (neocarzinostatin) or three-base (calicheamicin) 3′ extensions (Zien et al., 1988; Povirk et al., 1988; Kappen et al., 1988). The large distance between the two sugars attacked in formation of the bleomycin-induced double-strand breaks would appear to exclude such a double-radical mechanism, even if formation of a double radical from bleomycin were possible.

It is intriguing that the difference in the stagger of the double-strand breaks induced by bleomycin and neocarzinostatin is reflected in the action of these drugs at sites of extrahelical bulges [see Williams and Goldberg (1988)]. Comparison of the actions of the two drugs on these and other substrates may eventually provide important clues to the stereochemistry of drug binding, particularly the possible role of chromophore intercalation in positioning the active site of the drugs for attack on specific sugars in the minor groove.

Biological Implications. There is considerable indirect evidence that double-strand breaks play a critical role in bleomycin-induced cytotoxicity (Taylor et al., 1979; Povirk, 1983), although other factors, such as production of toxic base propenals, have also been suggested (Grollman et al., 1985). In any case, the repairability of bleomycin-induced double-strand breaks is an important issue. Studies with transfected DNA have shown that, in mammalian cells, double-strand breaks with normal (5′-phosphate and 3′-hydroxyl) termini are efficiently rejoined, usually without the loss of a single terminal base (Roth & Wilson, 1986). Such simple rejoining of bleomycin-induced double-strand breaks would be prevented by the phosphoglycolate moieties blocking all 3′ termini. Whether this presents a serious impediment to repair is unknown, but it is clear that additional processing is required, and the efficiency of such processing may be critically dependent on the exact geometry of the termini.

Using supercoiled DNA, we recently showed that in addition to double-strand breaks, bleomycin also induces an almost equal number of abasic sites with closely opposed breaks (Povirk & Houlgrave, 1988). Attempts to determine the sequence specificity of these lesions are in progress; however, since abasic sites and strand breaks are believed to result from partitioning of the same C-4′ deoxyribose free radical intermediate (Wu et al., 1985), it would not be surprising if the sequence specificity of abasic sites with closely opposed breaks was similar to that of double-strand breaks. Thus, it is notable that blunt-ended double-strand breaks were formed with high frequency at each of the two most prominent hot spots for bleomycin-induced mutagenesis in the *c*I gene, i.e., sites 2 and 11 in Figure 3, which share the sequence C-G-*C*-C (Povirk, 1987). If bleomycin also produced, at these sites, analogous lesions consisting of an abasic site plus a strand break (with one-base gap) directly opposite, they would be expected to be highly mutagenic lesions, since coding information would be lost at the same sequence position in both DNA strands.

ACKNOWLEDGMENTS

We thank W. T. Bradner and Bristol Laboratories for providing bleomycin.

Registry No. Bleomycin A_2, 11116-31-7; Fe(III) bleomycin, 72028-04-7.

REFERENCES

Burger, R. M., Peisach, J., & Horwitz, S. B. (1981) *J. Biol. Chem. 256*, 11636.
Cameron, V., & Uhlenbeck, D. (1977) *Biochemistry 16*, 5120.
D'Andrea, A. D., & Haseltine, W. A. (1978) *Proc. Natl. Acad. Sci. U.S.A. 75*, 3608.
Giloni, L., Takeshita, M., Johnson, F., Iden C., & Grollman, A. P. (1981) *J. Biol. Chem. 256*, 8608.
Grollman, A. P., Takeshita, M., Pillai, K. M., & Johnson, F. (1985) *Cancer Res. 45*, 1127.
Hecht, S. M. (1986) *Acc. Chem. Res. 19*, 383.
Hutchinson, F., & Povirk, L. F. (1979) in *Bleomycin: Chemical, Biochemical, and Biological Aspects* (Hecht, S. M., Ed.) Springer-Verlag, New York.
Kappen, L. S., Chen, C., & Goldberg, I. H. (1988) *Biochemistry 27*, 4331.
Keller, T. L., & Oppenheimer, N. J. (1987) *J. Biol. Chem. 262*, 15144.
Kuo, M. T., & Haidle, C. W. (1974) *Biochim. Biophys. Acta 335*, 109.
Kuramochi, H., Katsuoshi, T., Takita, T., & Umezawa, H. (1981) *J. Antibiot. 34*, 576.
Lloyd, R. S., Haidle, C. W., & Robberson, D. L. (1978a) *Biochemistry 17*, 1890.
Lloyd, R. S., Haidle, C. W., & Hewitt, R. R. (1978b) *Cancer Res. 38*, 3191.
Lloyd, R. S., Haidle, C. W., & Robberson, D. L. (1979) *Gene 7*, 303.
Maniatis, T., Fritsch, E. F., & Sambrook, J. (1982) *Molecular Cloning*, Cold Spring Harbor Laboratory, Cold Spring Harbor, NY.
Maxam, A. M., & Gilbert, W. A. (1980) *Methods Enzymol. 65*, 499.
Mirabelli, C. K., Ting, A., Huang, C.-H., Mong, S., & Crooke, S. T. (1982) *Cancer Res. 42*, 2779.
Padbury, G., Sligar, S. G., Labeque, R., & Marnett, L. J. (1988) *Biochemistry 27*, 7846.
Povirk, L. F. (1979) *Biochemistry 18*, 3989.
Povirk, L. F. (1983) in *Molecular Aspects of Anti-cancer Drug Action* (Neidle, S., & Waring, M., Eds.) pp 157–181 MacMillan, London.
Povirk, L. F. (1987) *Mutat. Res. 180*, 1.
Povirk, L. F., & Houlgrave, C. W. (1988) *Biochemistry 27*, 3850.
Povirk, L. F., Wübker, W., Köhnlein, W., & Hutchinson, F. (1977) *Nucleic Acids Res. 4*, 3573.
Povirk, L. F., Houlgrave, C. W., & Han, Y.-H. (1988) *J. Biol. Chem.* (in press).
Roth, D. B., & Wilson, J. H. (1986) *Mol. Cell. Biol. 6*, 4295.
Takeshita, M., Grollman, A. P., Ohtsubo, E., & Ohtsubo, H. (1978) *Proc. Natl. Acad. Sci. U.S.A. 75*, 5983.
Takeshita, M., Grollman, A. P., Ohtsubo, E., & Ohtsubo, H. (1978) *Proc. Natl. Acad. Sci. U.S.A. 75*, 5983.
Takeshita, M., Kappen, L. S., Grollman, A. P., Eisenberg, M., & Goldberg, I. H. (1981) *Biochemistry 20*, 7599.

Taylor, A. M. R., Rosney, C. M., & Campbell, J. B. (1979) *Cancer Res. 39*, 1046.
Williams, L. D., & Goldberg, I. H. (1988) *Biochemistry 27*, 3004.
Wu, J. C., Kozarich, J. W., & Stubbe, J. (1985) *Biochemistry 24*, 7562.
Zien, N., Sinha, A. M., McGahren, W. J., & Ellestad, G. A. (1988) *Science 240*, 1198.

Synthesis and Characterization of 5-[(4-Azidophenacyl)thio]uridine 5′-Triphosphate, a Cleavable Photo-Cross-Linking Nucleotide Analogue†

Michelle M. Hanna,* Suzanne Dissinger, Bradley D. Williams, and James E. Colston

Department of Biological Chemistry, California College of Medicine, University of California, Irvine, Irvine, California 92717

Received January 30, 1989; Revised Manuscript Received March 23, 1989

ABSTRACT: The synthesis, isolation, and characterization of a new photo-cross-linking uridine 5′-triphosphate analogue are described. This nucleotide analogue, 5-[(4-azidophenacyl)thio]uridine 5′-triphosphate (5-APAS-UTP), contains an aryl azide group approximately 10 Å from the uridine ring. The azide is photoactivated by irradiation at 300 nm, resulting in covalent attachment of the nucleotide to adjacent molecules. The nucleotide can be desulfurated with Raney nickel to cause molecular cleavage between the base and the aryl azide. Desulfuration yields uridine 5′-triphosphate and *p*-azidoacetophenone. If the analogue is cross-linked to another molecule, desulfuration leaves the analogue's acetophenone group attached to that molecule. This effectively leaves behind a molecular tag on molecules that interact with the uridine analogue either as monomeric nucleotide or as part of an RNA molecule. This nucleotide analogue can be incorporated into internal positions in RNA by transcription in vitro with *Escherichia coli* RNA polymerase. It can therefore be used to examine interactions between RNA and other molecules (e.g., proteins or nucleic acids). Because the sulfur atom can be selectively removed, the covalent bonds formed between analogue-containing RNA and other molecules can be cleaved, when desired, to facilitate identification of the cross-linked molecules and RNA nucleotides in the cross-linked complex.

Photochemical cross-linking is a powerful tool for the characterization of RNA–protein or RNA–nucleic acid interactions that occur during biological processes. Although there are a number of approaches one can take to photo-cross-linking of RNA, one of the most selective involves the incorporation of nucleotide analogues containing photoreactive cross-linking groups into the RNA molecule. Irradiation with ultraviolet or visible light converts these chemically inert groups to chemically reactive species that can covalently bond to adjacent molecules.

A number of nucleotide analogues have been characterized that have different cross-linking groups, excitation maxima, distances between the nucleotide and the cross-linker, and cross-linker position on the nucleotide (base, sugar, or phosphate) [for review, see Hanna (1988)]. Many of these contain photoreactive aryl azides as the cross-linking functional group. The half-life of the photolytically produced reactive species, the nitrene, is on the order of a millisecond, and its insertion reactions are highly nonspecific (Knowles, 1972; Bayley & Knowles, 1977; Schrock & Schuster, 1984). This nonspecificity is particularly useful when the environment of a protein or nucleic acid is probed, as there need not be a specific functional group within contact of the nitrene to get cross-linking.

Two types of azide-tagged nucleotide analogues containing cleavable bonds function as transcription initiation substrates for *Escherichia coli* RNA polymerase. These have been used to examine the interactions between the 5′ end of an RNA molecule and the RNA polymerase catalyzing its synthesis (Grachev & Zaychikov, 1981; Hanna & Meares, 1983a,b; Bernhard & Meares, 1986a,b; Stackhouse & Meares, 1988). However, many molecular interactions between RNA molecules and proteins or nucleic acids involve internal RNA sequences that can only be probed by incorporation of photo-cross-linking nucleotides within the RNA chain.

Three photo-cross-linking analogues that have been transcriptionally incorporated in vitro into RNA and used for RNA–protein cross-linking at internal uridine residues are 4-thio-UTP (Cramer et al., 1971; Bartholomew et al., 1987; Tanner et al., 1988), 5-bromo-UTP (Tanner et al., 1988), and 5-azido-UTP (Evans & Haley, 1987; Woody et al., 1988). All of these analogues have their cross-linking groups attached directly to the uridine base, allowing only close molecular contacts with the RNA to be examined. None of these analogues contains cleavable bonds.

We describe here the synthesis of a new UTP analogue that contains an aryl azide approximately 10 Å from the uridine which can be rapidly photoactivated by irradiation with long-wavelength ultraviolet light (300 nm). The azide group makes this analogue useful not only for examining RNA–protein interactions but RNA–DNA and RNA–RNA interactions as well. In addition, this analogue contains a sulfur atom between the nucleotide and the cross-linking group which

† Supported by an American Cancer Society grant (NP-544) and an Irvine Faculty Research Award to M.M.H. and NIH Predoctoral Training Grant GM07134-14 to S.D.

* Correspondence should be addressed to this author.

0006-2960/89/0428-5814$01.50/0